Catalysis Science & Technology

This article can be cited before page numbers have been issued, to do this please use: M. Hosseini-Sarvari, F. jafari, A. Mohajeri and N. Hassani , *Catal. Sci. Technol.*, 2018, DOI: 10.1039/C8CY00822A.

View Article Online
DOI: 10.1039/C8CY00822A

Journal Name

ARTICLE

Cu_2O/TiO_2 nanoparticles as visible light photocatalyst concerning $C(sp^2)$-P bond formation

Received 00th January 20xx,
Accepted 00th January 20xx

DOI: 10.1039/x0xx00000x

www.rsc.org/

Mona Hosseini-Sarvari,* Fattaneh Jafari, Afshan Mohajeri, and Nasim Hassani

A novel and efficient method has been developed for the construction of aromatic-phosphorus (Ar-P) bond formation by using Cu_2O/TiO_2 nanoparticles as inexpensive and available photocatalyst, under visible light irradiation. This protocol aspects simple system without use of any base, ligand, oxidant, and special conditions. This is the first report for the synthesis of aryphosphonates from arylhydrazines in visible light irradiation.

Introduction

From 1900, which $Ph_3C^{\bullet}$ radical was discovered, the chemistry of organic radicals began.[1] In all these years, significant advances have been made in organic radicals chemistry.[2-4] Nowadays, enormous activities have been done in radical chemistry which relies on photo redox catalysis used for generation of radical species. From 2007, MacMillan and after many other researchers disclosed a new term in this chemistry and using organo or organometallic photocatalysts under visible light for a wide range of organic synthesis.[5-8] In comparison between traditional redox and photoredox catalysis, generally photo redox catalysis improved the aspects of green chemistry (avoid using stoichiometric toxic initiators). In addition, photoredox catalyst could absorb visible light instead of organic molecules and so various photochemical reactions could be successfully performed under visible light irradiation. Ruthenium(II), Iridium(III)- base complexes, and organic dyes are the commonly and, mostly photocatalyst which these days were used in organic synthesis.[9-11] However, they are very expensive, toxic and also homogeneous catalysts. So, replace these expensive photocatalysts with a new series of inexpensive, heterogeneous, and more available photocatalyst are very important. Based on our interest in metal oxides, mixed metal oxides, and metal doped metal oxides over the last 10 years,[12-15] we focused our new projects on the development of new systems for photoredox catalytic reactions.[16,17],

TiO_2 has been known for many years as a photocatalyst.[18, 19] However, the main drawback of this metal oxide is its large band gap (Rutile TiO_2, Eg = 3.0 eV and Anatase TiO_2, Eg = 3.2 eV), so, it only could absorb the light under UV region. There are many modifications reported in the literature to improve its photocatalytic activity, which could absorb visible light (400-700 nm).[20-31] In addition, after TiO_2 absorb electromagnetic with E> Eg, electrons transfer from valence band (VB) into conduction band (CB) of TiO_2 and electron-hole pairs (e^-, h^+) generate. Rapid recombination of these e^-, h^+ pairs is another drawback of TiO_2. composites have been widely studied and used in many scopes.[18, 32-36] Cuprous oxide (Cu_2O) is a *p*-type semiconductor with narrow bandgap (2.0 eV) which has capability for absorption light in visible region.[37, 38] Previously the Cu_2O/TiO_2 system was reported as a good photocatalyst.[39-42] However, to the best of our knowledge there are no report for this semiconductor composite (Cu_2O/TiO_2) as a photocatalyst in organic synthesis. Pure TiO_2 has no photo activity in visible light, however Cu_2O could adsorb the visible light and generate e^-, h^+ pairs. These photogenerated electrons could transfer to CB of TiO_2, so the recombination of e^-, h^+ were suppressed. Finally, the electrons in CB of TiO_2 and holes in VB of Cu_2O have reduction, and oxidation ability, respectively, and they can interfere in photocatalytic system.

Phosphin oxides and arylphosphonates have been known as important organic compound owing to their widely uses in pharmaceuticals, biochemistry, agrochemistry, organic chemistry and also catalysis.[43-52] Hence, many new and catalytic methods for their synthesis have been reported.[53-58] Among all methods, new methods for Csp^2-P bond formation in the area of visible light photoredox catalysis have been developed.[59-62] However, in comparison with formation of C-C and C-X (O, N, and S) bonds using photo redox catalysis,[63-67] C-P and P-X bonds formation under visible light stay less explored.[60-62, 68] Based on the library studies there are only one method published for the synthesis of arylphosphonates using visible light irradiation, contain using aryldiazonium salt, and aryl halides as precursors (Scheme 1). Therefore, this is the first example for Csp^2-P bond formation using arylhydrazines as precursor under visible light irradiation using a nano semiconductor composite as a photoredox catalyst (Scheme 1).

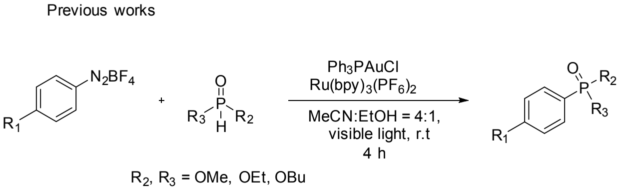

He, Wu, & Toste, 2015

---

aDepartment of Chemistry, Faculty of Science, Shiraz University, Shiraz, 7194684795 I.R. Iran; E-mail: hossaini@shirazu.ac.irElectronic Supplementary Information (ESI) available: [details of any supplementary information available should be included here]. See DOI: 10.1039/x0xx00000x

View Article Online
DOI: 10.1039/C8CY00822A

This work

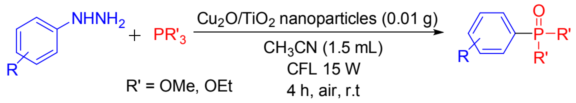

Scheme 1. Synthesis of arylphosphonates

Results and Discussion

Characterization of Cu_2O/TiO_2 nanoparticles

First to figure out the content of Cu and Ti in the catalyst, it was dissolved in concentrated H_2SO_4 and then analyzed by inducted coupled plasma (ICP) analysis. The results were shown that the amount of Cu and Ti were 30.06% (w/w) and 6.27% (w/w), respectively.

Figure 1a, shows the crystal structure and composition of TiO_2, Cu_2O, and Cu_2O/TiO_2 nanoparticles, respectively. Five Cu_2O diffraction peaks at 29.87˚, 36.48˚, 42.37˚, 61.45˚ and 73.51˚ (PDF card No. 05-0667)[69], can be indexed in XRD pattern of Cu_2O/TiO_2 nanoparticles. No diffraction peaks belonging to TiO_2 were observed indicating the high dispersion of TiO_2 on Cu_2O. This is agreed with ICP analysis. The crystal size of Cu_2O is about 34 nm, which was determined by Sherrer equation from 2Θ = 36.48˚diffraction peak.

SEM and TEM of the synthesized Cu_2O/TiO_2 nanoparticles is represented in Figure 1b, and 1c. Spherical particles could be clearly seen, with wide range of size. The size is approximately between 10-50 nm measuring from both SEM and TEM.

The FT-IR spectra of the catalyst is displayed in Figure 2. The peak at 632 cm^{-1} belongs to the Cu-O bond,[70] and absorptions at about 550 cm^{-1} is ascribed to the characteristic absorption band of Ti-O-Ti.[71-73] The broad absorption at 1620 and 3440 cm^{-1} are belong to the bending vibration of H-O-H bond vibration and the stretching vibration of the adsorbed water molecules, respectively.

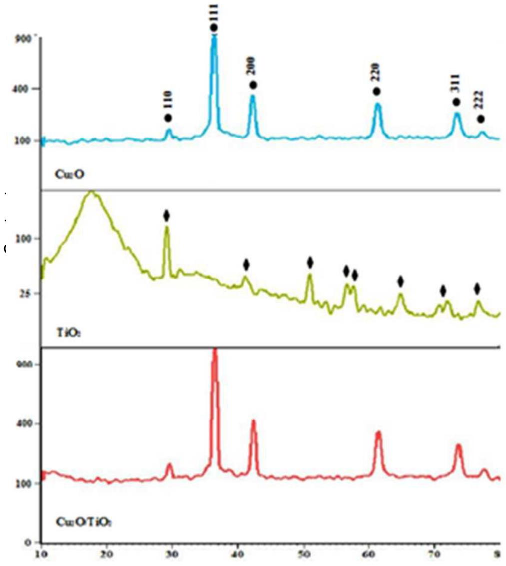

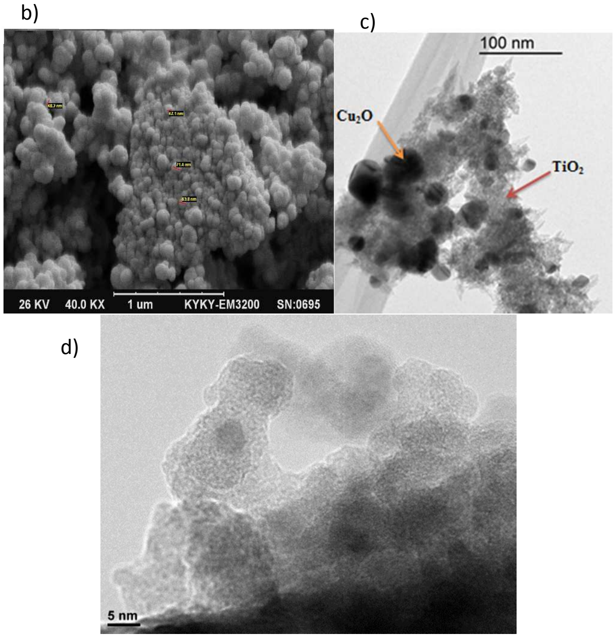

Figure 1. a) The XRD pattern, b) SEM, c) TEM, and d) HR-TEM images of Cu_2O/TiO_2 nanoparticles.

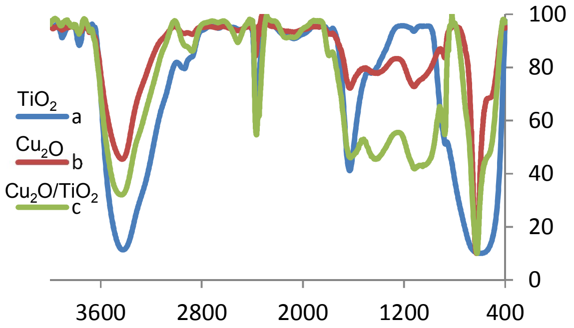

Figure 2. FT-IR spectrum of a) TiO_2, b) Cu_2O, and c) Cu_2O/TiO_2 nanoparticles.

BET measurements of Cu_2O/TiO_2 nanoparticles and its data is shown in Table 1. The BET surface area and BJH adsorption surface area of pores of Cu_2O/TiO_2 nanoparticles were detected to be 32.663 m²/g, and 39.282 m²/g, respectively. The single point total pore volume and the pore diameter were found to be 0.091 cc/g, and 3.891 nm, respectively.

Table 1. Results of BET surface area measurements for nano Cu_2O/TiO_2 photocatalyst.

BJH adsorption summary	
Surface Area	39.282 m²/g
Pore Volume	0.091 cc/g
Pore Diameter Dv(d)	3.891 nm
BJH desorption summary	
Surface Area	47.576 m²/g
Pore Volume	0.093 cc/g

View Article Online
DOI: 10.1039/C8CY00822A

Pore Diameter Dv(d)	3.766 nm
BET summary	
Surface Area	32.663 m²/g

Finally, to find the optical characteristics of catalyst, the UV-Vis absorption measurements were performed and the spectrum displayed in Figure 3. It is clear that the Cu_2O and Cu_2O/TiO_2 nanoparticles could be excited by visible light, whereas TiO_2 exhibited the absorption at belonging to the ultraviolet light range. The combination of these two metal oxide can increase the absorbance in long wavelength range. This assists and improves photo generated carrier transfer and charge separation, respectively. The *Eg* of Cu_2O/TiO_2 nanocomposite is about 2.76, which was determined by $E=h^*C/\lambda_{max}$ from λ_{max}=449 nm.[74]

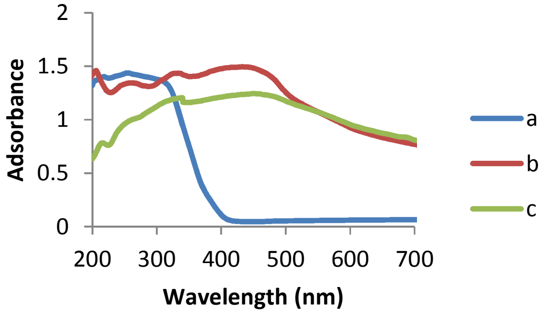

Figure 3. UV–vis diffuse reflection absorption spectra of a) TiO_2, b) Cu_2O, and c) Cu_2O/TiO_2 nanoparticles.

Coupling of arylhydrazine and trialkylphosphite under visible light over the nano Cu_2O/TiO_2 photocatalyst

We began our consideration into a visible light Csp^2-P bond formation reaction with phenylhydrazine and triethylphosphite in CH_3CN and Cs_2CO_3 in the presence of Cu_2O/TiO_2 nanoparticles as photocatalyst, and from this initial reaction the corresponding diethylphenyl phosphonate **3a** was produced in 91% yield (Scheme 2).

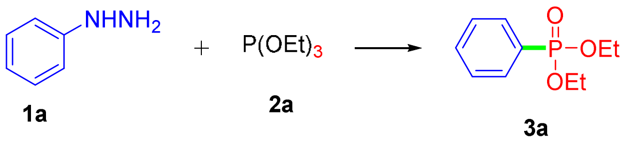

Scheme 2. Coupling of phenylhydrazine and triethylphosphite.

Then to improve the reaction condition different factors were investigated. To check the solvent effect, the above model reaction was performed in some chosen solvents such as DMF, DMSO, toluene, THF, MeOH, EtOAc, and 1,4-dioxane under visible light irradiation. According to the Table 2, acetonitrile was shown the best result (entry 1), toluene and 1,4-dioxan was shown with lower yields (entries 2, 3). MeOH and EtOAc were shown 65-70% yields (entries 4, 5) and also THF was shown poor yield (entry 6) and with DMF and DMSO the photocatalyst lost its efficiency and no product was observed (entry 7, 8). In addition, solvent-free condition was not afforded any product (entry 9).

Table 2. Optimization of solvent[a]

Entry	Solvent	Yield (%)[b]
1	CH_3CN	91
2	Toluene	86
3	1, 4 dioxane	82
4	MeOH	69
5	EtOAc	67
6	THF	36
7	DMF	Trace
8	DMSO	Trace
9	Neat	Trace

a) *Reaction conditions*: Phenylhydrazine (1.0 mmol), diethylphosphite (1.0 mmol), Cs_2CO_3 (3.0 mmol), Cu_2O/TiO_2 nanoparticles (0.01 g), solvent (1.5 mL), under CFL 12 W white for 4 h. b) Isolated yield.

During our optimization studies, some bases were also examined such as Cs_2CO_3, tributhylamine, K_3PO_4, NaO^tBu and KOH (Table 3). From Table 3, Cs_2CO_3 was shown as the best base (Table 3, entry 1), whereas tributhylamine and K_2CO_3 rendered lower yield (Table 3, entry 2, 3). K_3PO_4 had good yield (Table 3, entry 4), but ^{t}BuONa and KOH did not render any product (Table 3, entry 5, 6), respectively. The reaction was also investigated under base free condition. The reaction underwent to generate the corresponding arylphosphonates without use of any base in high yield. So, all the C-P bond formation reactions were achieved under base-free conditions.

Table 3. Optimization of base [a]

Entry	Base	Yield (%)[b]
1	Cs_2CO_3	91
2	Tributhylamine	84
3	K_2CO_3	84
4	K_3PO_4	81
5	NaO^tBu	Trace
6	KOH	Trace
7	-	94

a) *Reaction conditions:* Phenylhydrazine (1.0 mmol), diethylphosphite (1.0 mmol), and Cu_2O/TiO_2 nanoparticles (0.01 g), base (3.0 mmol), in CH_3CN (1.5 mL), under CFL 15 W white for 4 h. b) Isolated yield.

According to Table 4, nano Cu_2O/TiO_2 particles (was establised to be the most potent photocatalyst in terms of reaction rate, and isolated yield. With respect to the photocatalyst loading, 0.01 g of Cu_2O/TiO_2 nanoparticles (34/1 molar ratio) was found to be optimal. When 0.005 g of Cu_2O/TiO_2 nanoparticles were used, the reaction did not go to completion and side product (biphenyl, which was isolated and identified and also was confirmed by GC-Mass) was observed (Table 4, entry 2). However, no serious development

View Article Online
DOI: 10.1039/C8CY00822A

was observed with 0.02 g of Cu_2O/TiO_2 nanoparticles and again side products (biphenyl) was observed (Table 4, entry 3). Different amount of Cu_2O was also checked and the result are presented in entries 4-6. No product was observed without use of any photocatalyst (Table 4, entry 10)

Table 4. Investigation of the photocatalytic activity[a]

Entry	Catalyst (g)	Yield (%)[b]
1	Nano Cu_2O/TiO_2 particles (0.01)[c]	94
2	Nano Cu_2O/TiO_2 particles (0.005)[c]	79
3	Nano Cu_2O/TiO_2 particles (0.02)[c]	82
4	Nano Cu_2O/TiO_2 particles (0.01)[d]	88
5	Nano Cu_2O/TiO_2 particles (0.01)[e]	81
6	Nano Cu_2O/TiO_2 particles (0.01)[f]	82
7	Nano Cu_2O particles (0.01)[g]	38
8	Nano TiO_2 particles (0.01)[g]	0
9	TiO_2 (p25) (0.01)[g]	trace
10	None[g]	0

a) Reaction conditions: Phenylhydrazine (1.0 mmol), diethylphosphite (1.0 mmol), and catalyst in CH_3CN (1.5 mL), under CFL 15 W white for 4 h. b) Isolated yield. c) The catalyst contains 6 mol% TiO_2. d) The catalyst contains 7 mol% TiO_2. e) The catalyst contains 9 mol% TiO_2. f) The catalyst contains 20 mol% TiO_2. g) After 24 h.

We also investigated four kinds of light. The process was carried out under white, blue, green, red and also in dark condition. The results are shown in Table 5. The same results were obtained by using white and green light so for convenience and availability we choose white light. Small amount of product 3a (21%) was observed in dark condition (This small amount of product preparation could be catalyzed by Cu(I)).[54] Even after three days no improvement in yield was observed. After three days the reaction was exposed to light and after 4h the reaction was completed. So, light is required for this reaction.

Table 5. Optimization of light[a]

Entry	Light	Yield (%)[b]
1	CFL white 12 W	94
2	Blue LED 12 W	83
3	Green LED 12W	94
4	Red LED 12 W	68
5	Dark	21[c]

a) *Reaction conditions:* Phenylhydrazine (1.0 mmol), diethylphosphite (1.0 mmol), and Cu_2O/TiO_2 nanoparticles (0.01 g) in CH_3CN (1.5 mL) for 4 h. b) Isolated yield. c) The reaction was performed for three days.

Finally, we tested the effect of the atmosphere on reaction. The reaction was accomplished under air, Ar, and O_2 conditions. The results are shown in Table 6.

At the end, from Tables 2-6 it can be seen that the best result was achived with Cu_2O/TiO_2 nanoparticles (0.01 g), in CH_3CN under CFL 15W white in air.

Table 6. Optimization of atmosphere [a]

Entry	Atmosphere	Yield (%)[b]
1	Air	94
2	Ar	43
3	O_2	95

a) *Reaction conditions:* Phenylhydrazine (1.0 mmol), triethylphosphite (1.0 mmol), and Cu_2O/TiO_2 nanoparticles (0.01 g) in CH_3CN (1.5 mL) under CFL 15 W white for 4 h. b) Isolated yield.

The reusability of the nano Cu_2O/TiO_2 photocatalyst was also investigated and the results are outlined in Figure 4. To recover the catalyst, it was centrifuged after completion of each cycle of the reaction and washed by diethylether. No remarkable loss of the catalytic activity was observed even after six cycles. In addition, XRD pattern and SEM of the recovered catalyst after six cycle in compare to the fresh catalyst (Figure 1a, b) was not shown any significant changes.

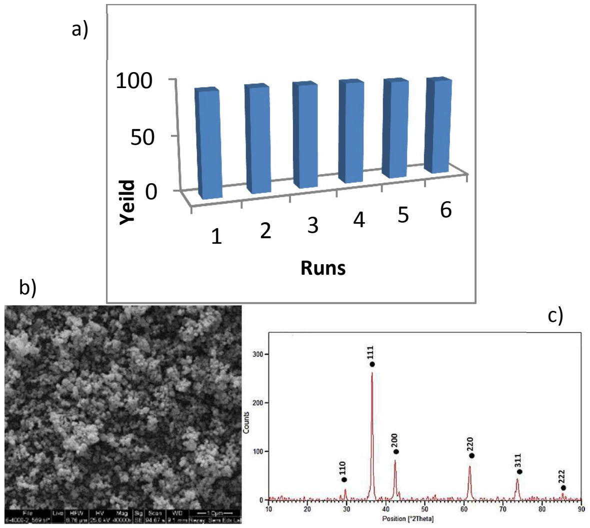

Figure 4. a) Reusability of the recovered catalyst in coupling of phenylhydrazine and triethylphosphite, b) SEM imag, and c) XRD pattern of the Cu_2O/TiO_2 nanoparticles after six cycle.

Some of substituted arylhydrazine derivatives and trialkylphosphite as the substrate were investigated in this C-P bond formation reaction, as shown in Table 7. The coupling reactions were well, and the desired products were isolated in excellent yields. No any homocoupling products were observed.

Table 7. C-P bond formation of arylhydrazine and trialkylphosphite by using nano Cu_2O/TiO_2 photocatalyst

View Article Online
DOI: 10.1039/C8CY00822A

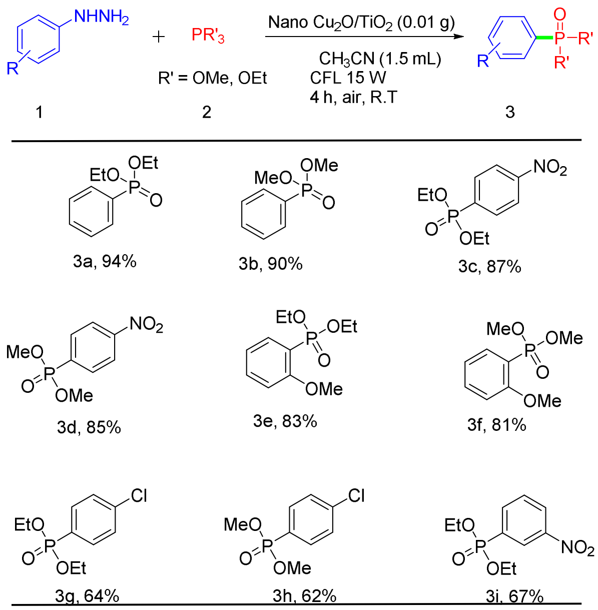

[a]*Reaction conditions*: Arylylhydrazine (1.0 mmol), trialkylphosphite (1.0 mmol), and Cu$_2$O/TiO$_2$ nanoparticles (0.01 g) in CH$_3$CN (1.5 mL) under CFL 15 W white. [b] Isolated yield.

The study suggests the mechanism:

To insights into reaction mechanism some control experiments were investigated as shown in Scheme 3. By adding a radical scavenger (TEMPO) to the reaction mixture under standard conditions, the desired arylphosphonate was obtained in a trace amount. Also in another experiment, triethanolamine (TEA) as a hole scavenger was added and in this case, again the desired product was obtained in trace amount. These results confirmed that the reaction is likely to involve a radical process. Moreover, when P(OPh)$_3$ was used as phosphonylation reagent instead of P(OEt)$_3$, it was decomposed into phenol and the corresponding product **3g** was not observed. So aryl radicals were contemplated as intermediate.

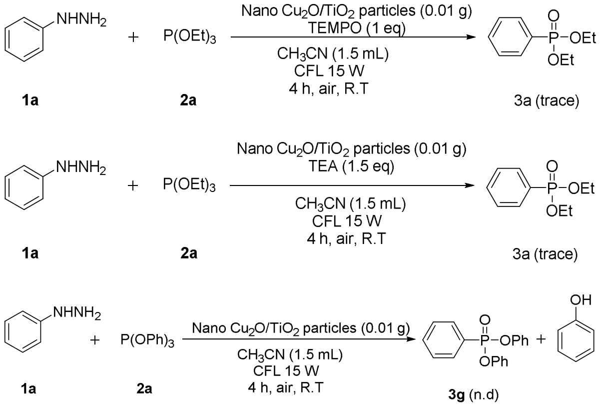

Scheme 3. Control experiments

Based on these results, a possible mechanism was proposed for nano Cu$_2$O/TiO$_2$ catalyzed photo P-Csp^2 bond formation (Figure 5). When nano Cu$_2$O/TiO$_2$ was irradiated by a CFL white lamp in a visible region (400 nm) only Cu$_2$O was excited and e$^-$/h$^+$ pairs were generate. The conduction band of Cu$_2$O(CB) is above of CB of TiO$_2$ so the generated electron transfer to CB of TiO$_2$.[42] This could prevent the recombination of e$^-$/h$^+$ pairs (Figure 5, a). This electron reacted with O$_2$ to generate the superoxide radical anion O$_2^{\cdot-}$. Further, phenylhydrazine react with O$_2^{\cdot-}$ and undergoes fragmentation to release aryl radical, nitrogen and hydrogen gases, and HO$_2^-$ (Figure 5, b).[75] Then the aryl radical was reacted with trialkylphosphite to generate an unstable phosphoraryl radical.[76] In continue, an ethyl radical release and the desired product was generated. The most reactive ethyl radical could transfer an electron to the hole (h$^+$) and formed a cation which could abstract a proton from HO$_2^-$. The reaction was investigated by GC and GC-MS analysis but the detection of ethane, H$_2$, and N$_2$ gas by our instruments (GC and GC-MS analysis) because of their low boiling points (lower than 30˚C) was not possible at the present.

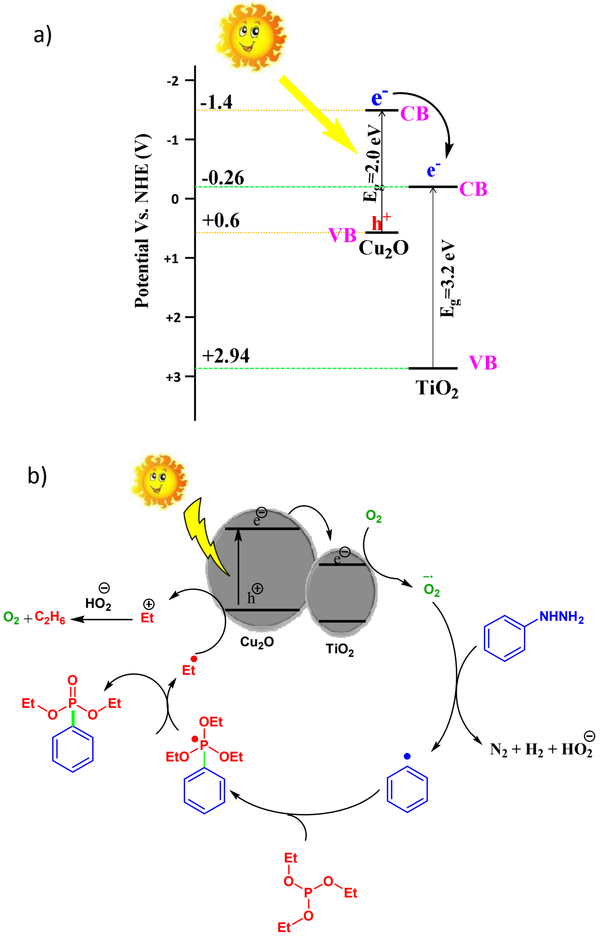

Figure 5. A) Potential diagram of Cu$_2$O and TiO$_2$,[77] B) proposed mechanism for synthesis arylphosphonates catalyzed by nano Cu$_2$O/TiO$_2$ photocatalyst under visible light illustration.

Theoretical calculations

View Article Online
DOI: 10.1039/C8CY00822A

To gain more insights into the reaction mechanism for synthesis of arylphosphonates, we performed density functional theory (DFT) calculation by the use of Gaussian 09 suite of programs.[78] All the structures were optimized at the B3LYP/6-311G(d) level of theory. Harmonic frequency calculations were performed at the same level to ensure that there are no imaginary frequencies for the minima and only one imaginary frequency for the transition state. Moreover, the self-consistent reaction field (SCRF) theory[79] was used for modeling the solvent (acetonitrile) effect, Zero point energies and thermodynamic functions were calculated at 298.15 K and 1 atm.

As discussed above, when $P(OPh)_3$ was used as phosphonylation reagent the arylphosphonate product was not observed. In order to probe the difference between $P(OPh)_3$ and $P(OEt)_3$ we briefly compare their electronic properties. Figure 6 shows the optimized structures together with the frontier molecular orbitals of $P(OPh)_3$ and $P(OEt)_3$ molecules. It can be seen that in the $P(OEt)_3$ the highest occupied molecular orbital (HOMO) and the lowest unoccupied molecular orbital (LUMO) are mostly localized on the phosphorus atom. In contrast, the LUMO of $P(OPh)_3$ is localized on the phenyl groups. The calculated energy gaps between the HOMO and LUMO orbitals are 2.89 and 1.36 eV for $P(OPh)_3$ and $P(OEt)_3$ molecules, respectively, which suggest higher reactivity for $P(OEt)_3$. It has been shown that, the most strongly binding site for an electron donor (electron acceptor) is where LUMO (HOMO) of the molecules farthest.[80] As shown in Figure 6, the LUMO of $P(OEt)_3$ is more protruding in comparison with that of $P(OPh)_3$ indicating that $P(OEt)_3$ can adsorb the electron donor species such as aryl radical more strongly than the $P(OPh)_3$.

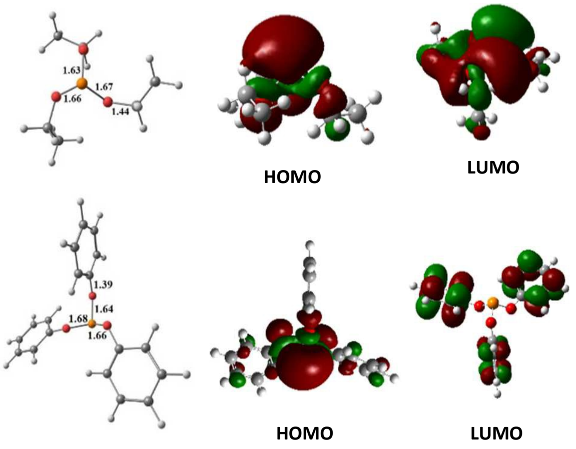

Figure 6. Optimized structure of the $P(OEt)_3$ and $P(Oph)_3$ together with the spatial distributions of their frontier molecular orbitals. Bond distances are given in angstrom. P, C, O, and H atoms are shown in orange, gray, red, and white, respectively.

To obtain further mechanistic details for the synthesis of arylphosphonate we have calculated the reaction energy profile for the reaction between $P(OEt)_3$ and aryl radical. The energy profile and the corresponding atomic configurations at various states along the reaction path are displayed in Figure 7. The process is exothermic by 1.35 eV, but a barrier of 0.48 eV should be overcome due to the breaking of the C-O bond and the formation of Ar-P bond. We have selected the $P(OEt)_3$ + aryl as initial state (**IS**). When aryl approaches the $P(OEt)_3$, a metastable intermediate (**IM**) is formed in which the phosphorous atom is four coordinated. In **IM**, the Ar-P bond distance is 1.88 Å and the configuration is 0.42 eV lower in energy than **IS**. The reaction proceed by crossing a barrier of 0.48 eV via passing over a transition state (**TS**). Figure 7 shows that, in **TS** configuration, the O–Et bond is elongated to 1.82 Å, while the Ar-P bond is shortened to 1.75 Å. The final state (**FS**) consists of arylphosphonate together with an ethyl radical. To enable the oxidation of ethyl, the VB of Cu_2O must be at an energy above that corresponding to the redox potential of ethyl radical. The edge of VB for Cu_2O was estimated to be at 0.6 V[9a] and the redox potential of ethyl that we calculated at G2 level of theory is 0.26 V. Thus, the electron transfer from ethyl radical into VB of Cu_2O is sufficiently energetic.

Finally, it is worth mentioning that when trying to obtain the energy profile for the $P(OPh)_3$, the reaction stopped by the repulsive interaction between $P(OPh)_3$ and aryl radical which is in agreement with our experimental observation.

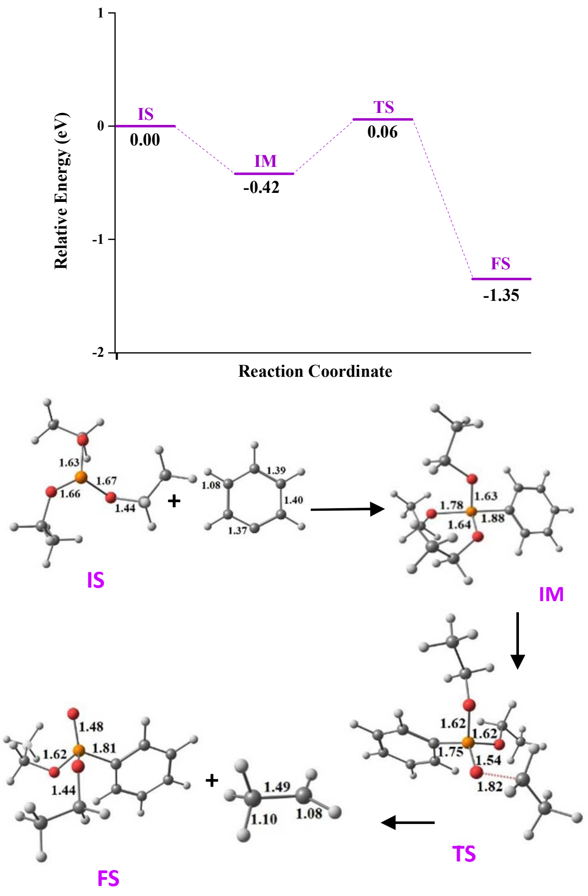

View Article Online
DOI: 10.1039/C8CY00822A

Figure 7. Energy profile and the structures of corresponding species along the reaction path for the $P(OEt)_3$+aryl. The bond lengths are given in angstrom. P, C, O, and H atoms are shown in orange, gray, red, and white, respectively.

Experimental Section

Preparation of Cu_2O/TiO_2 nanoparticles[81]

Cu_2O/TiO_2 nanostructure composite oxides were formed by the modified subsequent method. 13.2 g (0.066 mol) of cupric acetate monohydrate was dissolved in 600 mL of distilled water, then addition of 3.2 mL (0.011 mol) of PEG-300 under vigorous stirring. Subsequently, 0.7 g (0.002 mol) of tetrabutyl titanate digested with ethanol (2-3 mL, Merck) was added drop by drop into the solution of cupric acetate. So, a white precipitate was produced during the mixing. Afterward, 5mL of 5 M NaOH and 15 mL of 5 M hydrazine were added dropwise consecutively into this slurry under energetic stirring, and the resulting mixture was hold onto 12–14°C for 15 min. An orange precipitate was then formed. It was centrifuged, washed with distilled water to neutral and further 3 times washed with acetone. The sample was then stay at 200°C for 3 h in oven then in 40°C for 24 h in vacuum oven. By this amount the sample was contained 6 mol% Ti and 30.06 mol% Cu. A series of Cu_2O/TiO_2 composite oxides were prepared in this way with different molar ratios of TiO_2 and Cu_2O. We prepared 7, 9, and 20 molar percentage of TiO_2 in Cu_2O/TiO_2, respectively.

General procedure for the synthesis arylphosphonates under visible light irradiation

Arylhydrazine (1 mmol), trialkylphosphite (1 mmol) CH_3CN (1.5 mL) and nano Cu_2O/TiO_2 photocatalyst (0.01 g, contain 0.048 mmol Cu and 0.0131 mmol Ti) were stirred at room temperature in air under visible light irradiation (CFL 15 W) until it was completed (4 h). Afterward, the reaction mixture was diluted with diethyl ether (10-15 mL), and centrifuged to separate the photocatalyst, and the solution was evaporated. The residue was purified by column chromatography on silica gel (petroleum ether/ethyl acetate 5:1 to 2:1) to afford desired pure product.

Conclusions

A novel way to the synthesis of arylphosphonates from arylhydrazine by using a nano photocatalyst has been reported. This is the first report using arylhydrazines as starting material to generate aryl radical for the synthesis of arylphosphonates under visible light irradiation. This method has experimental simplicity, very short reaction time at room temperature, easy work-up, base, ligand and oxidant free. We believe that this new photoredox C-P bond formation using a visible light reaction could be find many applications in pharmaceutical, academic, and industrial research.

Acknowledgements

This work was supported by Shiraz University Research Council.

Notes and references

1. M. Gomberg, *J. Am. Chem. Soc.*, 1902, 24, 597-628.
2. C. P. Jasperse, D. P. Curran and T. L. Fevig, *Chem. Rev.*, 1991, 91, 1237-1286.
3. S. Kumar, Y. Kumar, S. K. Keshri and P. Mukhopadhyay, *Magnetochemistry.*, 2016, 2, 42.
4. M. Yan, J. C. Lo, J. T. Edwards and P. S. Baran, *J. Am. Chem. Soc.*, 2016, 138, 12692-12714.
5. D. A. Nicewicz and D. W. C. MacMilla, *Science.*, 2008, 322, 77-80.
6. J. M. R. Narayanam, J. W. Tucker and C. R. J. Stephenson, *J. Am. Chem. Soc*, 2009, 131, 8756-8757.
7. M. A. Ischay, M. E. Anzovino, J. Du and T. P. Yoon, *J. Am. Chem. Soc*, 2008, 130, 12886-12887.
8. M.-Q. Yang and Y.-J. Xu, *Phys. Chem. Chem. Phys.*, 2013, 15, 19102-19118.
9. T. Koike and M. Akita, *Inorg. Chem. Front.*, 2014, 1, 562-576.
10. K. Teegardin, J. I. Day, J. Chan and J. Weaver, *Org. Process Res. Dev.*, 2016, 20, 1156-1163.
11. C. K. Prier, D. A. Rankic and D. W. C. MacMillan, *Chem. Rev.*, 2013, 113, 5322-5363.
12. M. Hosseini-Sarvari, A. Khanivar and F. Moeini, *J. Mater. Sci.*, 2015, 50, 3065-3074.
13. M. Hosseini-Sarvari, T. Ataee-Kachouei and F. Moeini, *RSC Adv.*, 2015, 5, 9050-9056.
14. M. Hosseini-Sarvari and Z. Razmi, *Appl. Surf. Sci.*, 2015, 324, 265-274.
15. M. Hosseini-Sarvari and F. Moeini, *New J. Chem.*, 2014, 38, 624-635.
16. M. Koohgard and M. Hosseini-Sarvari, *Catal. Commun.*, 2018, 111, 10-15.
17. M. Hosseini-Sarvari and Z. Bazyar, *Chem. Select*, 2018, 3, 1898-1907.
18. R. Fagan, D. E. McCormack, D. D. Dionysiou and S. C. Pillai, *Mater. Sci. Semicond. Process.*, 2016, 42, 2-14.
19. H. Kazuhito, I. Hiroshi and F. Akira, *Jpn. J. Appl. Phys.*, 2005, 44, 8269.
20. Z. Luo, H. Jiang, D. Li, L. Hu, W. Geng, P. Wei and P. Ouyang, *RSC Adv.*, 2014, 4, 17797-17804.
21. Y. Bessekhouad, D. Robert and J.-V. Weber, *Catal. Today.*, 2005, 101, 315-321.
22. N. Rahimi, R. A. Pax and E. M. Gray, *Prog. Solid State Chem.*, 2016, 44, 86-105.
23. H. Y He, *Micro and Nanosystems.*, 2011, 3, 14-25.
24. W.-K. Jo and T. Sivakumar Natarajan, *ACS Appl. Mater. Interfaces*, 2015, 7, 17138-17154.
25. L. Wang, J. Shen, S. Yang, W. Liu, Q. Chen and M. He, *Green Chem.*, 2018, 20, 1290-1296.
26. J. Tang, G. Grampp, Y. Liu, B.-X. Wang, F.-F. Tao, L.-J. Wang, X.-Z. Liang, H.-Q. Xiao and Y.-M. Shen, *J. Org. Chem.*, 2015, 80, 2724-2732.
27. L. Wang, C. Wang, W. Liu, Q. Chen and M. He, *Tetrahedron Lett.*, 2016, 57, 1771-1774.
28. L. Wang, Y. Wang, Q. Chen and M. He, *Tetrahedron Lett.*, 2018, 59, 1489-1492.
29. W. Liu, C. Wang and L. Wang, *Ind. Eng. Chem. Res.*, 2017, 56, 6114-6123.

View Article Online
DOI: 10.1039/C8CY00822A

30. W. Liu, C. Wang, Y. Huang, Q. Chen, L. Wang and M. He, *Synth. Commun.*, 2016, 46, 1268-1274.
31. B. Wang, J. Durantini, J. Nie, A. E. Lanterna and J. C. Scaiano, *J. Am. Chem. Soc.*, 2016, 138, 13127-13130.
32. A. K. Tripathi, M. C. Mathpal, P. Kumar, M. K. Singh, S. K. Mishra, R. K. Srivastava, J. S. Chung, G. Verma, M. M. Ahmad and A. Agarwal, *Mater. Sci. Semicond. Process.*, 2014, 23, 136-143.
33. W. Gao, R. dos Reis, L. T. Schelhas, V. L. Pool, M. F. Toney, K. M. Yu and W. Walukiewicz, *Nano Lett.*, 2016, 16, 5247-5254.
34. H. Yan, X. Wang, M. Yao and X. Yao, *Prog. Natural Sci.: Mat. Inter.*., 2013, 23, 402-407.
35. V. Binas, D. Venieri, D. Kotzias and G. Kiriakidis, *J. Materiomics.*, 2017, 3, 3-16.
36. L. G. Devi and R. Kavitha, *Appl. Catal. B.*, 2013, 140-141, 559-587.
37. P. E. de Jongh, D. Vanmaekelbergh and J. J. Kelly, *Chem. Comm.*, 1999, DOI: 10.1039/A901232J, 1069-1070.
38. X. Lin, R. Zhou, J. Zhang and X. Sheng, *Mater. Sci. Poland.*, 2010, 28, 504--511.
39. Y. Li, B. Wang, S. Liu, X. Duan and Z. Hu, *Appl. Surf. Sci.*, 2015, 324, 736-744.
40. L. Yang, S. Luo, Y. Li, Y. Xiao, Q. Kang and Q. Cai, *Environ. Sci. Technol.*, 2010, 44, 7641-7646.
41. M. Wang, L. Sun, Z. Lin, J. Cai, K. Xie and C. Lin, *Energy Environ. Sci.*, 2013, 6, 1211-1220.
42. L. Huang, F. Peng, H. Wang, H. Yu and Z. Li, *Catal. Commun.*, 2009, 10, 1839-1843.
43. Y. Li, L.-Q. Lu, S. Das, S. Pisiewicz, K. Junge and M. Beller, *J. Am. Chem. Soc.*, 2012, 134, 18325-18329.
44. J.-J. Shie, J.-M. Fang, S.-Y. Wang, K.-C. Tsai, Y.-S. E. Cheng, A.-S. Yang, S.-C. Hsiao, C.-Y. Su and C.-H. Wong, *J. Am. Chem. Soc*, 2007, 129, 11892-11893.
45. J.-L. Montchamp, *Acc. Chem. Res.*, 2013, 47, 77-87.
46. C. S. Demmer, N. Krogsgaard-Larsen and L. Bunch, *Chem. Rev.*, 2011, 111, 7981-8006.
47. L. D. Quin, *A guide to organophosphorus chemistry*, John Wiley & Sons, 2000.
48. S. Van der Jeught and C. V. Stevens, *Chem. Rev.*, 2009, 109, 2672-2702.
49. D. S. Surry and S. L. Buchwald, *Angew. Chem. Int. Ed.*, 2008, 47, 6338-6361.
50. A. Skarżyńska, *Coord. Chem. Rev.*, 2013, 257, 1039-1048.
51. J. Galezowska and E. Gumienna-Kontecka, *Coord. Chem. Rev.*, 2012, 256, 105-124.
52. Q. Dang, Y. Liu, D. K. Cashion, S. R. Kasibhatla, T. Jiang, F. Taplin, J. D. Jacintho, H. Li, Z. Sun and Y. Fan, *J. Med. Chem.*, 2010, 54, 153-165.
53. H. Luo, H. Liu, X. Chen, K. Wang, X. Luo and K. Wang, *Chem. Commun.*, 2017, 53, 956-958.
54. S.-Y. Chen, R.-S. Zeng, J.-P. Zou and O. T. Asekun, *J. Org. Chem.*, 2014, 79, 1449-1453.
55. W. C. Fu, C. M. So and F. Y. Kwong, *Org. Lett.*, 2015, 17, 5906-5909.
56. M.-T. Chen, X. You, L.-G. Bai and Q.-L. Luo, *Org. Biomol. Chem.*, 2017, 15, 3165-3169.
57. S. Sobhani and Z. Ramezani, *RSC Adv.*, 2016, 6, 29237-29244.
58. M. Khrizanforov, S. Strekalova, K. Kholin, V. Khrizanforova, M. Kadirov, T. Gryaznova and Y. Budnikova, *Catal. Today.*, 2017, 279, 133-141.
59. P. Peng, L. Peng, G. Wang, F. Wang, Y. Luo and A. Lei, *Org. Chem. Front.*, 2016, 3, 749-752.
60. R. S. Shaikh, S. J. Düsel and B. König, *ACS Catal.*, 2016, 6, 8410-8414.
61. Y. He, H. Wu and F. D. Toste, *Chem. Sci.*, 2015, 6, 1194-1198.
62. J. Xuan, T. T. Zeng, J. R. Chen, L. Q. Lu and W. J. Xiao, *Chem. Eur. J.*, 2015, 21, 4962-4965.
63. G. Pandey, R. Laha and D. Singh, *J. Org. Chem.*, 2016, 81, 7161-7171.
64. H. Sagir, P. Rai, A. Ibad, F. Ibad and I. R. Siddiqui, *Catal. Commun.*, 2017, 100, 153-156.
65. D. Xia, Y. Li, T. Miao, P. Li and L. Wang, *Green Chem.*, 2017, 19, 1732-1739.
66. L. Zhang, J. Zhu, J. Ma, L. Wu and W.-H. Zhang, *Org. Lett.*, 2017, 19, 6308-6311.
67. W. Huang and P. L. Diaconescu, *Inorg. Chim. Acta.*, 2012, 380, 274-277.
68. D. P. Hari and B. König, *Org. Lett.*, 2011, 13, 3852-3855.
69. L. Liu, W. Yang, Q. Li, S. Gao and J. K. Shang, *ACS Appl. Mater. Interfaces.*, 2014, 6, 5629-5639.
70. D. Liu, S. Yang and S.-T. Lee, *J. Phys. Chem. C.*, 2008, 112, 7110-7118.
71. M. Hosseini-Sarvari, E. Sodagar and M. M. Doroodmand, *J. Org. Chem.*, 2011, 76, 2853-2859.
72. F. Nemati, M. M. Heravi and A. Elhampour, *RSC Adv.*, 2015, 5, 45775-45784.
73. T. Xin, M. Ma, H. Zhang, J. Gu, S. Wang, M. Liu and Q. Zhang, *Appl. Surf. Sci.*, 2014, 288, 51-59.
74. J. Dharma, A. Pisal and C. Shelton, *Application Note Shelton, CT: PerkinElmer.*, 2009.
75. T. S. Calderwood, C. L. Johlman, J. L. Roberts Jr, C. L. Wilkins and D. T. Sawyer, *J. Am. Chem. Soc.*, 1984, 106, 4683-4687.
76. J.-J. L. Fu and W. G. Bentrude, *J. Am. Chem. Soc.*, 1972, 94, 7710-7717.
77. J. Fu, S. Cao and J. Yu, *J. Materiomics.*, 2015, 1, 124-133.
78. M. J. e. a. Frisch, *Gaussian 09, revision A.02; Gaussian, Inc.: Wallingford, CT*, 2009.
79. M. W. Wong, M. J. Frisch and K. B. Wiberg, *J. Am. Chem. Soc.*, 1991, 113, 4776-4782.
80. S. Chrétien, S. K. Buratto and H. Metiu, *Curr. Opin. Solid St. Mat. Sci.*, 2007, 11, 62-75.
81. C. Han, Z. Li and J. Shen, *J. Hazard. Mater.*, 2009, 168, 215-219.

View Article Online
DOI: 10.1039/C8CY00822A

Cu_2O/TiO_2 nanoparticles as visible light photocatalyst concerning C (sp^2)-P bond formation

Mona Hosseini-Sarvari,* Fattaneh Jafari, Afshan Mohajeri, and Nasim Hassani